Optical fabrication of the MMT adaptive secondary mirror

H. M. Martin[a], J. H. Burge[a], C. Del Vecchio[b], L. R. Dettmann[a], S. M. Miller[a], B. Smith[a] and F. Wildi[a]

[a]Steward Observatory, University of Arizona, Tucson, AZ 85721
[b]Osservatorio Astrofisico di Arcetri, L.go E. Fermi 5, 50125 Firenze, Italy

ABSTRACT

We describe the optical fabrication of the adaptive secondary mirror for the MMT. The 640 mm f/15 secondary consists of a flexible glass shell, 1.8 mm thick, whose shape is controlled by 336 electromagnetic actuators. It is designed to give diffraction-limited images at a wavelength of 1 micron. For generating and polishing, the shell was supported by attaching it to a rigid glass blocking body with a thin layer of pitch. It could then be figured and measured using techniques developed for rigid secondaries. The highly aspheric surface was polished with a 30 cm stressed lap and small passive tools, and measured using a swing-arm profilometer and a holographic test plate. The goal for fabrication was to produce diffraction-limited images in the visible, after simulated adaptive correction using only a small fraction of the typical actuator forces. This translates into a surface accuracy of less than 19 nm rms with correction forces of less than 0.05 N rms. We achieved a surface accuracy of 8 nm rms after simulated correction with forces of 0.02 N rms.

Keywords: telescopes, optical fabrication, optical testing, adaptive optics

1. THE MMT ADAPTIVE SECONDARY MIRROR

The adaptive optics system for the 6.5 m MMT is based on an adaptive secondary mirror designed to give diffraction-limited images in the near-infrared, between 1 and 5 microns.[1,2] With the adaptive correction applied at the secondary mirror, the system introduces no unnecessary warm reflections, and provides a corrected wavefront to any instrument placed at the f/15 Cassegrain focus.

The adaptive secondary mirror consists of a thin Zerodur shell, 1.8 mm thick and 640 mm in diameter, supported by 336 voice-coil actuators. Actuator forces are generated by electromagnets coupled to small permanent magnets, which are bonded to the back of the Zerodur shell. The actuators suspend the shell over a rigid glass reference surface. Capacitive sensors measure the gap (nominally 50 microns) between the two surfaces and allow each actuator to maintain closed-loop position control. The narrow air gap provides crucial viscous damping to the system. A flexure at the mirror's central hole supplies the lateral restraint.

The system will use both natural and sodium laser guide stars. The wavefront sensor for initial operation is a 12×12 Shack-Hartmann sensor. It provides feedback to control up to 120 natural modes of the thin mirror with a bandwidth of 750 Hz. Use of a higher-resolution wavefront sensor in the future will allow all 336 modes to be controlled.

2. ACCURACY REQUIREMENTS FOR FABRICATION

In operation, we expect the adaptive secondary to maintain a wavefront accuracy of about 75 nm rms, corresponding to diffraction-limited imaging at 1 micron. The mirror must be figured to an accuracy consistent with this goal. Errors in the polished figure, up to some amplitude, will be corrected by the actuators. We therefore set the goal for fabrication in terms of the wavefront accuracy after simulated adaptive correction of the static figure error. The forces required to correct this permanent error should be a small fraction of the forces needed in adaptive operation. In addition to the correction of static figure error, the operational forces include the weight of the shell, wind, and correction for the atmosphere. These are expected to sum to about 0.1 N rms per actuator in good conditions. The goal set for optical fabrication was to achieve a surface accuracy of 19 nm rms, after simulated adaptive correction using forces of less than 0.05 N rms.

In standard operation of the adaptive secondary mirror, the correction is based on the Shack-Hartmann wavefront sensor. With only 108 subapertures, its resolution is inadequate to measure and control all 336 actuators independently. Correction of static figure errors should involve all 336 degrees of freedom. For this we measure the mirror with a phase-shifting interferometer, whose resolution is roughly 300×300 pixels. The interferometer is part of the test bench that will be used for initial testing and debugging of the adaptive secondary system, and will be available for periodic testing in the telescope.[3] It includes optics which, with the secondary mirror, image a fiber point source to a point at the telescope's f/15 focus. It thus simulates a stellar image, including any aberrations introduced by the secondary. The light is then fed to the Shack-Hartmann wavefront sensor for system testing, and (through a beam splitter) to the interferometer for high-resolution measurements.

Allowing a simulated adaptive correction of the static figure error relaxes the accuracy requirement for the uncorrected figure. The relaxation is greatest for large-scale errors, which are easily corrected with small actuator forces. Small-scale errors must be controlled more completely by the figuring process because their adaptive correction requires large forces. On the scale of the actuator spacing (32 mm) and smaller scales, the accuracy depends almost entirely on the figuring process, which must therefore produce a very smooth surface.

Achieving small-scale smoothness is challenging for the f/15 secondary because of its severe asphericity. Working with a 6.5 m f/1.25 primary, the secondary is similarly fast and aspheric. The optical parameters are listed in Table 1.

Table 1. Optical parameters of the f/15 secondary mirror

diameter	640 mm
R	1795 mm
k	-1.409
p-v departure from best-fit sphere	82 microns surface

3. METHOD OF FABRICATION

The combination of high asphericity and tight specification for small-scale smoothness makes the f/15 secondary a challenging optic to manufacture, even apart from its flexibility. We polished it at the Steward Observatory Mirror Lab, using a system designed specifically for highly aspheric mirrors requiring very smooth surfaces. We have used this system to figure a number of large, stiff primary and secondary mirrors to accuracies of 15-30 nm rms surface error.[4,5] It involves a large, stiff polishing tool and substantial polishing loads, so could not be used for a thin flexible mirror without special consideration of mirror support. Our plan for the adaptive secondary was therefore to support the mirror so it would behave like a rigid mirror during fabrication. We could then use the proven techniques developed for large, stiff aspheres.

During fabrication, the mirror must be supported uniformly and with sufficient force to resist polishing loads of 1-2 kPa, or 25-50 times the weight of the mirror. It must also remain near its relaxed shape, for any strains induced by the support will be imprinted in the surface figure. The 336 actuators would not provide a sufficiently uniform support and in any case are not designed to resist such loads. We supported the mirror on a rigid substrate, bonded with a thin layer of pitch, the highly viscous, tar-like material used as a polishing medium and bonding agent in optical fabrication.

Figure 1 illustrates the general sequence of operations during fabrication of the secondary mirror. We first machined the Zerodur substrate to a thick meniscus "proto-shell", and machined another Zerodur substrate to a convex curve that matched the concave rear surface of the proto-shell. We lapped these surfaces together and attached them with a 100 micron layer of Gugolz 73 pitch. We then machined the proto-shell down to a thickness of about 2 mm. We used a nearly full-diameter rigid tool to lap the convex surface spherical, then grind in the 82 microns of aspheric departure.

Bonding with pitch provided a support that is stiff against polishing forces, while still allowing the glass to relax under internal stress that may change as most of the material is removed during the thinning process. Pitch is a visco-elastic material with elastic modulus in the range of plastics (on the order of 5 GPa) and very high viscosity (on the order of 10 Gpoise) at room temperature. Thus a thin layer adds little elastic compliance. The viscous flow potentially allows the glass to relax, but could also allow undesirable deformation under polishing loads. We determined through experiments that a thickness of about 100 microns would not allow significant deformations under the force of small polishing tools.[6] We do

expect the pitch to exert small stresses that distort the shell, but only in low-order bending modes. These will add to any static figure errors left by the polishing process and will be corrected by the actuators.

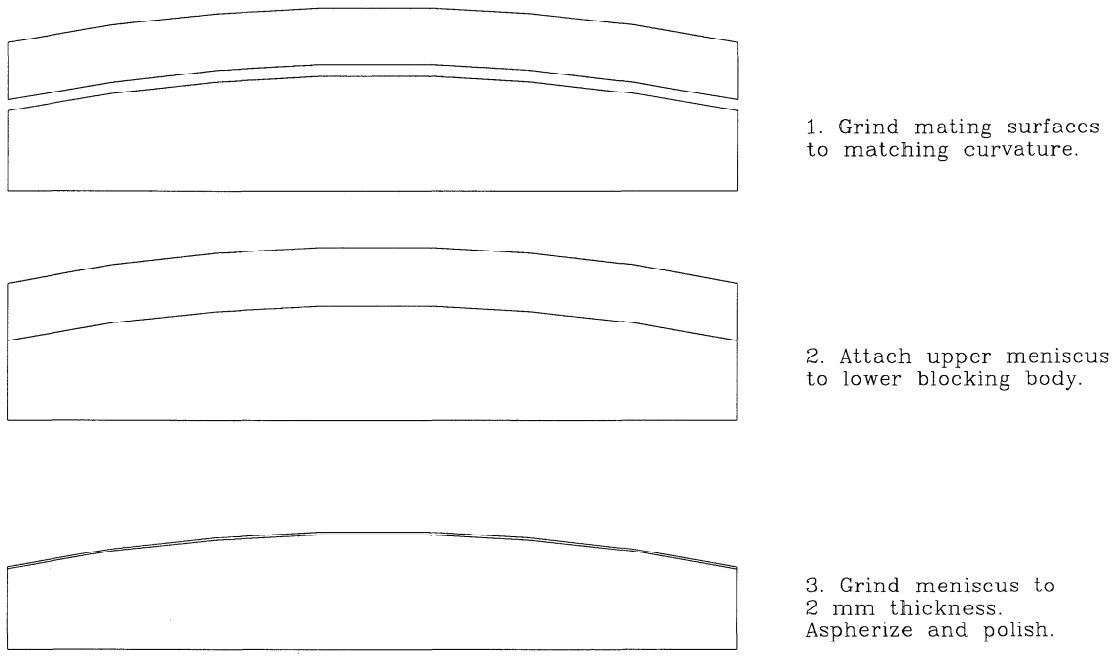

Figure 1. Steps in the optical fabrication of the adaptive secondary shell.

We polished and figured the mirror using a 30 cm actively stressed lap and small passive laps.[7,8] The stressed lap, shown in Figure 2, is bent elastically under computer control so that it always matches the local curvature of the mirror as it translates and rotates. This active control of the lap's shape allows use of a large and stiff lap, and hence gives a dramatic improvement in passive smoothing of small-scale structure. While a passive lap under controlled load naturally matches the local height, slope and average curvature of the mirror surface, the stressed lap also matches several higher-order varying curvature terms. These additional terms correspond to the low-order bending modes—focus, astigmatism and coma—of the lap shape. Good smoothing requires a shape error on the order of 1 micron or less between the lap and the mirror surface. In the presence of 80 microns of asphericity, matching the additional curvature terms in the surface shape allows the lap to be many times larger.

When the shell is figured to the desired accuracy, it is removed from the blocking body by heating the assembly to melt the pitch. Support and handling of the free shell are serious issues for shells larger than about 1 m diameter, but the adaptive secondary shell at 64 cm can be held at the edge and handled safely by one person.

4. METHOD OF TESTING

We measured the mirror with two methods, both developed at the Mirror Lab. We use a contact profilometer during aspherizing and the early polishing stages. The profilometer, shown in Figure 3, rotates around a bearing whose axis goes through the mirror's center of curvature, so the probe traces out an arc of the best fitting sphere.[9] The probe measures the departure from a spherical surface to an accuracy of better than 100 nm, as confirmed by comparison with optical tests.

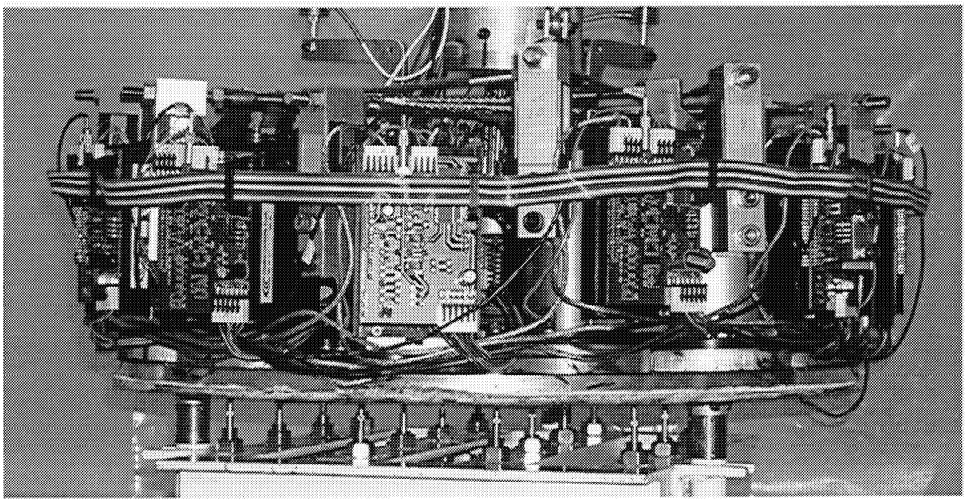

Figure 2. Stressed lap used to figure the adaptive secondary mirror. The lap is mounted on an array of displacement sensors that measure its shape changes for testing and calibration. The lap's aluminum plate, 45 cm in diameter and 13 mm thick, is visible below the bending actuators. The plate is faced with pitch over a 30 cm diameter to form the polishing surface.

The optical test used for final figuring and evaluation of the figure accuracy is made with a holographic test plate.[9] A full-diameter spherical test plate is manufactured, then a computer-generated hologram is written on the concave reference surface. The hologram is designed so that its first-order backward diffraction produces a reference wavefront that matches a perfect secondary mirror. The test wavefront passes through the hologram (zeroth-order), reflects off the secondary mirror, and returns through the hologram. The test plate is translated by PZTs to allow phase-shifting interferometry. The test is illuminated by a large aluminum reflector which, being common to both test and reference wavefronts, can have relatively low accuracy. Similarly, the test plate can have low transmission quality.

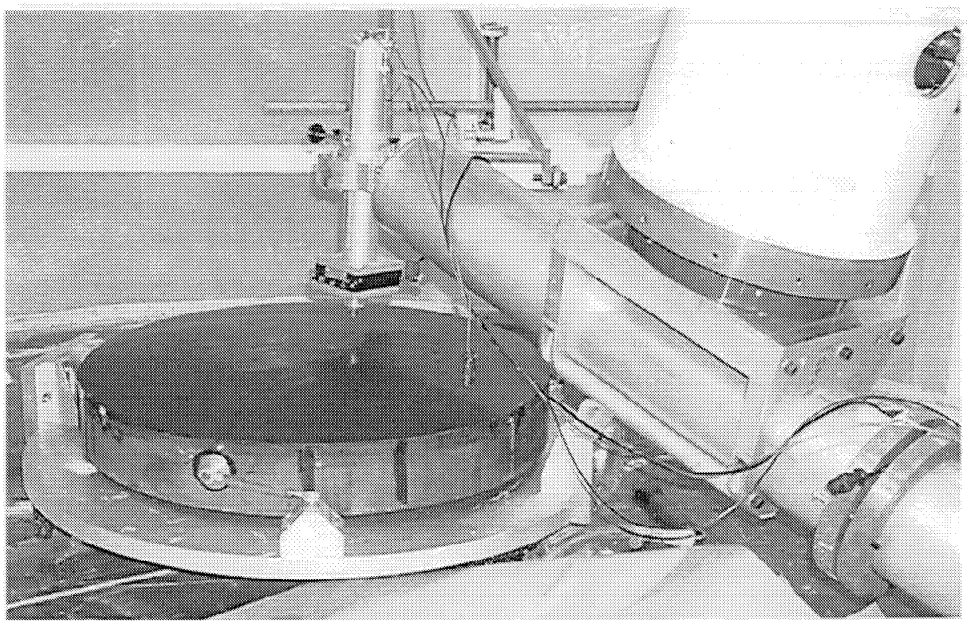

Figure 3. Adaptive secondary shell, bonded to a rigid blocking body, being measured with the profilometer. The cylinder at upper right is the profilometer's bearing, aligned with the mirror's center of curvature.

5. ANALYSIS AND RESULTS

As described above, we evaluated the figure accuracy by simulating adaptive correction of the figure errors. The simulation was based on the set of 336 actuator influence functions—surface displacements for a unit displacement of each actuator in turn—calculated by finite-element analysis. For each influence function, the analysis also gave the set of 336 forces required to give the unit displacement of one actuator and zero displacement of all others.

We performed a least-squares fit of the influence functions to the map of surface error obtained from the optical test. Figure 4 shows the measured surface error, the fit to the measured error, the residual fitting error, and a representation of the actuator forces. The uncorrected mirror has an accuracy of 73 nm rms surface error. The residual error after the fit is 8 nm rms. The actuator forces required to correct the figure are 0.02 N rms, with a maximum force of 0.07 N. The mirror therefore meets its requirements with more than a factor of 2 to spare in both wavefront accuracy and actuator force.

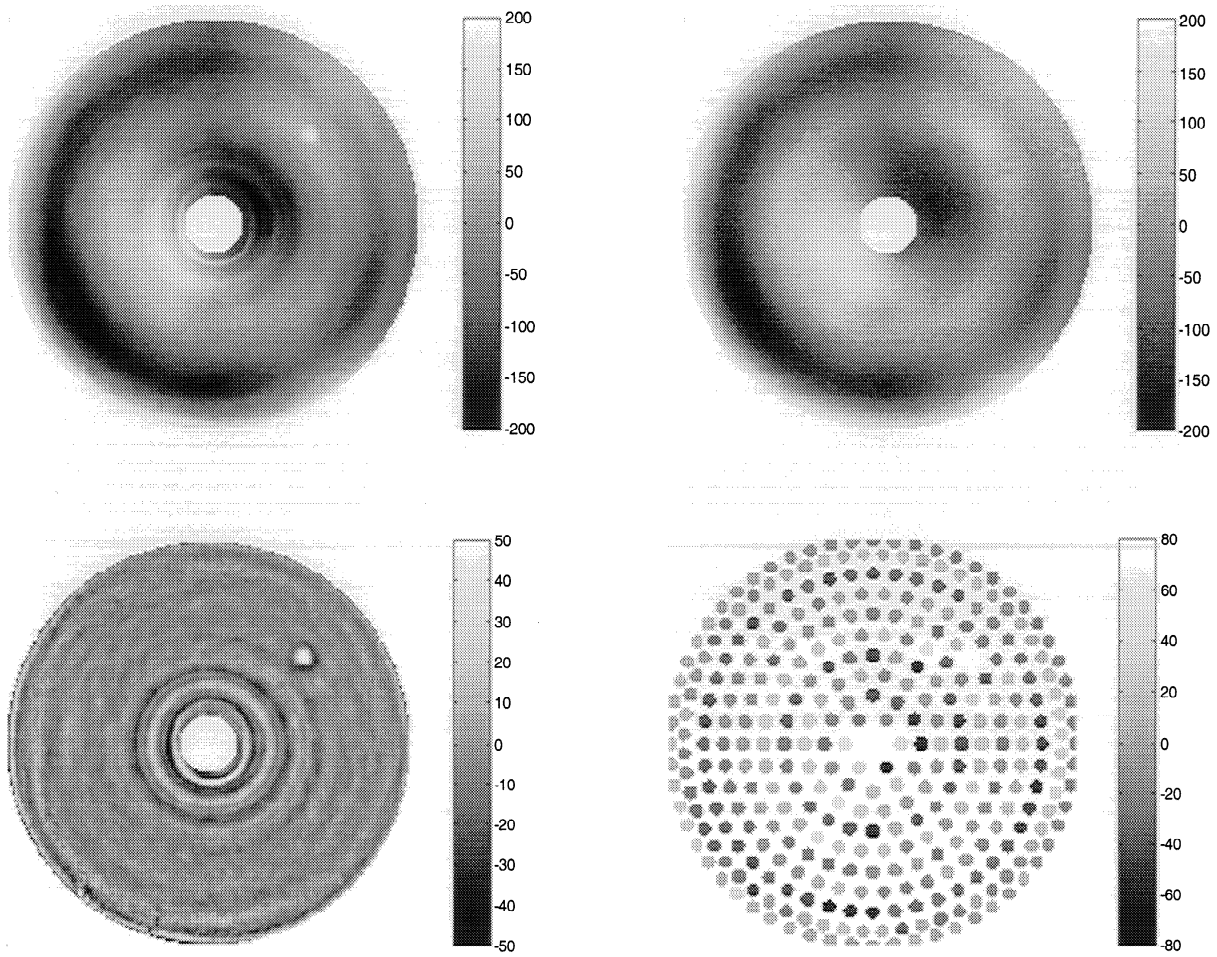

Figure 4. Upper left: surface figure of the adaptive secondary shell bonded to the blocking body. Upper right: fit of actuator influence functions to the secondary figure. Lower left: residual error. Lower right: actuator forces that produce the best fit; the correction forces are the negative of these. Gray-level bars are labeled in nm of surface error for the surface maps, and mN for the actuator force diagram.

The simulated correction almost completely removes the non-axisymmetric structure, which is all at scales large enough to be corrected by the actuators. The residual error is dominated by axisymmetric structure on a scale too small for complete correction. Its shape is determined by both the original error and the layout of actuators in 10 concentric rings. The most prominent feature, the small bump in the upper right quadrant, is caused by a cluster of small bubbles (<1 mm diameter) in the layer of pitch bonding the shell to the blocking body. We believe this is a case of quilting: the lack of support over the bubbles allowed the shell to deflect downward under the load of the lap. Polished smooth in this condition, the shell sprang back when the lap's load was removed, leaving a bump that is too narrow to be corrected well by the actuators. This feature illustrates the flexibility of the shell and its sensitivity to the support. In order to avoid such sensitivity to small support errors during the fabrication of future thin shells, we are exploring a modified technique in which the optical surface is figured first, before thinning the shell.

The adaptive secondary shell is still attached to its blocking body, while the actuator system is being tested with a dummy spherical shell. When these tests are complete we will mount the aspheric shell on the actuators, measure its figure, and perform the adaptive correction of the static figure error. The test bench also includes spinning "turbulence plates"—acrylic plates with Kolmogorov spectra of surface errors machined into their surfaces—to simulate atmospheric seeing. With this system we will perform dynamic tests and demonstrate closed-loop control of the adaptive secondary mirror before it goes to the telescope.

ACKNOWLEDGEMENTS

This work has been supported by the Air Force Office of Scientific Research under grant number F49620-99-1-0285.

REFERENCES

1. M. Lloyd-Hart, J. R. P. Angel, D. G. Sandler, T. K. Barrett, P. C. McGuire, T. A. Rhoadarmer, D. G. Bruns, S. M. Miller, D. W. McCarthy and M. Cheselka, "Infrared adaptive optics system for the 6.5-m MMT: system status and prototype results", in *Adaptive Optical System Technologies*, Domenico Bonaccini, Robert K. Tyson, Editors, Proc. SPIE 3353, p. 82 (1998).
2. P. Salinari and D. G. Sandler, "High-order adaptive secondary mirrors: where are we?", in *Adaptive Optical System Technologies*, Domenico Bonaccini, Robert K. Tyson, Editors, Proc. SPIE 3353, p. 742 (1998).
3. R. J. Sarlot and J. H. Burge, "Optical system for closed-loop testing of adaptive optic convex mirror", in *Novel Optical Systems and Large-Aperture Imaging*, Kevin D. Bell, Michael K. Powers, Jose M. Sasian, Editors, Proc. SPIE 3430 , p. 126 (1998).
4. B. K. Smith, J. H. Burge and H. M. Martin, "Fabrication of large secondary mirrors for astronomical telescopes", in *Optical Manufacturing and Testing II*, H. P. Stahl, Editor, Proc. SPIE 3134, p. 51 (1997).
5. H. M. Martin, R. G. Allen, J. H. Burge, L. R. Dettmann, D. A. Ketelsen, W. C. Kittrell and S. M. Miller, "Polishing of a 6.5 m f/1.25 mirror for the first Magellan telescope", in *Optical Fabrication and Testing*, Roland Geyl, Jonathan Maxwell, Editors, Proc. SPIE 3739, p. 47 (1999).
6. S. Miller, R. Angel, B. Martin, J. Kapp, D. Ketelsen and L. Dettmann, "Fabrication of ultra thin mirrors for adaptive and space optics", in *Adaptive Optics and Applications*, Robert K. Tyson, Robert Q. Fugate, Editors, Proc. SPIE 3126, p. 391 (1997).
7. H. M. Martin, D. S. Anderson, J. R. P. Angel, R. H. Nagel, S. C. West and R. S. Young, "Progress in the stressed-lap polishing of a 1.8-m f/1 mirror", in *Advanced Technology Optical Telescopes IV*, Larry D. Barr, Proc. SPIE 1236, p. 682 (1990).
8. S. C. West, H. M. Martin, R. H. Nagel, R. S. Young, W. B. Davison, T. J. Trebisky, S. T. DeRigne and B. B. Hille, "Practical Design and Performance of the Stressed Lap Polishing Tool", *Applied Optics*, **33**, p. 8094 (1994).
9. J. H. Burge, "Measurement of large convex aspheres", in *Optical Telescopes of Today and Tomorrow: Following in the Direction of Tycho Brahe*, Arne Ardeberg, Editor, Proc. SPIE 2871, p. 362 (1997).